

# Genetic ablation of smooth muscle $K_{IR2.1}$ is inconsequential to the function of mouse cerebral arteries

Paulina M Kowalewska<sup>1\*</sup> , Jacob Fletcher<sup>1\*</sup>,  
William F Jackson<sup>2</sup>, Suzanne E Brett<sup>1</sup>, Michelle SM Kim<sup>1</sup>,  
Galina Yu Mironova<sup>1</sup>, Nadia Haghbin<sup>1</sup>, David M Richter<sup>1</sup>,  
Nathan R Tykocki<sup>2</sup> , Mark T Nelson<sup>3</sup> and Donald G Welsh<sup>1</sup>

Journal of Cerebral Blood Flow & Metabolism  
2022, Vol. 42(9) 1693–1706  
© The Author(s) 2022



Article reuse guidelines:  
sagepub.com/journals-permissions  
DOI: 10.1177/0271678X221093432  
journals.sagepub.com/home/jcbfm



## Abstract

Cerebral blood flow is a finely tuned process dependent on coordinated changes in arterial tone. These changes are strongly tied to smooth muscle membrane potential and inwardly rectifying  $K^+$  ( $K_{IR}$ ) channels are thought to be a key determinant. To elucidate the role of  $K_{IR2.1}$  in cerebral arterial tone development, this study examined the electrical and functional properties of cells, vessels and living tissue from tamoxifen-induced smooth muscle cell (SMC)-specific  $K_{IR2.1}$  knockout mice. Patch-clamp electrophysiology revealed a robust  $Ba^{2+}$ -sensitive inwardly rectifying  $K^+$  current in cerebral arterial myocytes irrespective of  $K_{IR2.1}$  knockout. Immunolabeling clarified that  $K_{IR2.1}$  expression was low in SMCs while  $K_{IR2.2}$  labeling was remarkably abundant at the membrane. In alignment with these observations, pressure myography revealed that the myogenic response and  $K^+$ -induced dilation were intact in cerebral arteries post knockout. At the whole organ level, this translated to a maintenance of brain perfusion in SMC  $K_{IR2.1}^{-/-}$  mice, as assessed with arterial spin-labeling MRI. We confirmed these findings in superior epigastric arteries and implicated  $K_{IR2.2}$  as more functionally relevant in SMCs. Together, these results suggest that subunits other than  $K_{IR2.1}$  play a significant role in setting native current in SMCs and driving arterial tone.

## Keywords

Arterial spin-labeling MRI, cerebral blood flow, electrophysiology, myography, potassium channels

Received 19 September 2021; Revised 1 March 2022; Accepted 8 March 2022

## Introduction

Cerebral blood flow (CBF) is maintained by a network of resistance arteries that match red blood cell delivery with metabolic activity.<sup>1,2</sup> The vascular smooth muscle (VSM) layer translates vasoactive stimuli into diameter changes, allowing for precise tuning of blood flow needed for optimal brain function.<sup>3–5</sup> Smooth muscle cell (SMC) contractility is tightly coupled to intracellular  $[Ca^{2+}]$ , an essential secondary messenger that sets myosin light chain phosphorylation and consequently the extent of cross-bridge cycling.<sup>6</sup> The influx of extracellular  $Ca^{2+}$  is facilitated by voltage-gated  $Ca^{2+}$  channels (VGCCs), integral membrane proteins whose activity is coupled to arterial membrane potential ( $V_M$ ).<sup>7</sup> It is the balance of inward depolarizing currents and outward hyperpolarizing currents that determine  $V_M$  in smooth muscle. The latter is largely delivered

through membrane-embedded  $K^+$  channels, including voltage-gated ( $K_V$ ), ATP-sensitive ( $K_{ATP}$ ),  $Ca^{2+}$ -activated, and inwardly rectifying ( $K_{IR}$ ) channels.<sup>8</sup>

<sup>1</sup>Robarts Research Institute and the Department of Physiology & Pharmacology, University of Western Ontario, London, ON, Canada  
<sup>2</sup>Department of Pharmacology and Toxicology, Michigan State University, East Lansing, MI, USA

<sup>3</sup>Department of Pharmacology, University of Vermont, Burlington, VT, USA

\*These authors contributed equally to this work.

## Corresponding author:

Paulina M Kowalewska, 1151 Richmond St N, RRI 7260, London, ON N6A 5B7, Canada.  
Email: pkowale@uwo.ca

In cerebral arteries,  $K_{IR}$  channels are major contributors to myogenic tone development.<sup>9</sup> They exist as tetrameric assemblies of 4  $\alpha$ -subunits from the strong inwardly rectifying  $K_{IR2.x}$  subfamily, of which  $K_{IR2.1}$  is thought to be the predominant subunit in SMCs.<sup>10,11</sup>  $K_{IR}$  channels possess several unique electrical characteristics, including inward rectification at membrane potentials negative to  $E_K$ , potentiation by extracellular  $K^+$ , and rapid blockade by micromolar  $Ba^{2+}$ .<sup>12,13</sup> At a functional level, these properties enable  $K_{IR}$  channels to participate in  $K^+$ -induced dilation, vessel hyperpolarization, and hemodynamic force sensing.<sup>3,14,15</sup> Interestingly,  $K_{IR2.2}$  subunits have also been identified in cerebral vessels and are thought to form functional channels when heteromultimerized with  $K_{IR2.1}$ .<sup>15,16</sup> This knowledge raised a key question centered on the overall contribution of  $K_{IR2.1}$  to native currents and their control over cerebral arterial function. Early studies using a global knockout mouse<sup>10,17</sup> implied a dominant role for SMC  $K_{IR2.1}$  in setting arterial  $V_M$  and tone. While informative, it is noteworthy that experimentation was limited to neonates due to the lethality of global gene deletion. More recent advances in genomic techniques allow for generation of inducible tissue-specific knockouts; this, in turn, creates the ideal opportunity to pursue a deeper understanding of  $K_{IR2.1}$  in adult cerebral vasculature.

Building on prior work, this study used an adult tamoxifen-induced SMC-specific  $K_{IR2.1}$  knockout model to further explore this channel's role in cerebral arterial function. Experiments progressed from isolated cells to live animals, employing electrophysiology, immunofluorescence labeling, western blotting, vessel myography, and arterial spin-labeling magnetic resonance imaging (ASL-MRI). Contrary to expectations, we observed robust  $K_{IR}$  currents in SMCs isolated from control and knockout mice. Immunolabeling subsequently revealed that, while  $K_{IR2.1}$  expression was reduced by knockout, its apparent abundance was low in control animals in contrast to the  $K_{IR2.2}$  subunit. Myography next showed that the myogenic response and  $K^+$ -induced dilation remained intact in knockout mice. This  $K^+$ -induced dilation was sensitive to low  $Ba^{2+}$  concentration, a property consistent with the electrophysiological profile of  $K_{IR2.2}$  rather than  $K_{IR2.1}$ .<sup>16</sup> Without a significant change in tone with SMC  $K_{IR2.1}$  deletion, brain perfusion was unaffected in live mice, as observed by ASL-MRI. The electrophysiology, protein expression, and myography findings were further confirmed in a second vascular network—epigastric arteries. Taken together, these results indicate that inward  $K^+$  currents in cerebral arterial myocytes are likely derived from subunits other than  $K_{IR2.1}$ .

## Methods

### Animal model and ethical approval

All animal procedures followed regulations set by the Canadian Council of Animal Care and were approved by the University of Western Ontario Animal Care Committee (Protocol #2017-144). Colonies were maintained under constant room temperature and humidity environment with a 12-hr light/dark cycle and allowed ad libitum access to food and water. The colony of SMMHC-CreER<sup>T2</sup> male mice, strain B6.FVB-Tg(Myh11-cre/ERT2)1Soff/J, was derived from a colony at the University of Vermont (Burlington, VT, USA). The SMMHC-CreER<sup>T2</sup> mice, which express a Cre recombinase under control of the smooth muscle myosin, heavy polypeptide 11, smooth muscle (*Myh11*) promoter on the Y chromosome,<sup>18</sup> were crossed with floxed  $K_{IR2.1}$  mice (strain B6.Cg-Kcnj2<sup>tm1swz</sup>)<sup>19</sup> to produce tamoxifen-inducible SMC  $K_{IR2.1}^{-/-}$  male mice. Six-week-old mice were treated with tamoxifen by oral gavage (0.12 mg kg<sup>-1</sup> in corn oil; Sigma-Aldrich) once daily for 5 days to induce SMC-specific deletion of  $K_{IR2.1}$  via tamoxifen-mediated nuclear translocation of Cre recombinase (Figure S1). Non-induced Cre SMC mice (Cre carriers with the floxed  $K_{IR2.1}$  gene) served as control animals. ARRIVE guidelines for reporting animal research were followed.<sup>20</sup>

### Cerebral artery and smooth muscle cell isolation

SMC  $K_{IR2.1}^{-/-}$  mice were euthanized via CO<sub>2</sub> asphyxiation 2–3 months after tamoxifen treatment with age-matched controls. The brain was removed and placed in chilled phosphate-buffered solution (PBS; pH 7.4) containing (in mM): 137 NaCl, 2.7 KCl, 10 Na<sub>2</sub>HPO<sub>4</sub>, 1.8 KH<sub>2</sub>PO<sub>4</sub>, and 5 glucose. Cerebral and cerebellar arteries were carefully dissected and cleaned for single-cell and isolated-vessel experiments. Specifically, middle and posterior cerebral as well as cerebellar arteries were used for patch experiments and posterior cerebral and cerebellar arteries were used for myography work. Dissected arteries were enzymatically digested to yield isolated SMCs using a two-step process.<sup>21</sup> Briefly, vessel segments were placed in isolation medium containing (in mM): 60 NaCl, 80 sodium glutamate, 5 KCl, 2 MgCl<sub>2</sub>, 10 glucose, and 10 HEPES with 1 mg mL<sup>-1</sup> bovine serum albumin (pH 7.4), and chilled on ice for 10 minutes before the reaction began. Following an initial warming period (37°C, 10 minutes), vessels underwent a two-step digestion process: 1) a 6-minute incubation in isolation medium containing 0.9 mg mL<sup>-1</sup> papain and 1 mg mL<sup>-1</sup> dithiothreitol and 2) a 7-minute incubation

in isolation medium containing  $0.3 \text{ mg mL}^{-1}$  H-type collagenase, and  $0.7 \text{ mg mL}^{-1}$  F-type collagenase. Vessels were then thoroughly washed with ice-cold isolation medium and allowed to rest on ice for 30 minutes before disruption with a fire-polished pipette.

### Electrophysiology

Whole-cell patch clamp electrophysiology was used to measure  $\text{Ba}^{2+}$ -sensitive  $\text{K}_{\text{IR}}$  currents in isolated cerebral artery SMCs. Recording electrodes were pulled from borosilicate glass (Sutter Instruments) using a micropipette puller (Narishige PP-830), fire-polished (Narishige MF-830) and filled with pipette solution containing (in mM): 5 NaCl, 35 KCl, 100 K-gluconate, 1  $\text{CaCl}_2$ , 0.5  $\text{MgCl}_2$ , 10 HEPES, 10 EGTA, 2.5  $\text{Na}_2\text{-ATP}$ , and 0.2 GTP (pH 7.2). Whole-cell access was obtained by placing the pipette onto a cell and applying negative pressure until membrane rupture occurred. Cells were then voltage clamped at  $-50 \text{ mV}$  and equilibrated in a bath solution containing (in mM): 140 NaCl, 5 KCl, 0.5  $\text{MgCl}_2$ , 10 HEPES, 10 glucose, and 0.1  $\text{CaCl}_2$ . To stimulate  $\text{K}_{\text{IR}}$  activity, extracellular  $\text{K}^+$  was increased with bath solution containing (in mM): 60 KCl, 85 NaCl, 0.5  $\text{MgCl}_2$ , 10 HEPES, 10 glucose, and 0.1  $\text{CaCl}_2$  (pH 7.4). Voltage was then stepped to  $-100 \text{ mV}$  for 100 ms and subsequently ramped to  $+20 \text{ mV}$  at a rate of  $0.04 \text{ mV ms}^{-1}$ .  $\text{Ba}^{2+}$  ( $100 \mu\text{M}$ ), a selective inhibitor of  $\text{K}_{\text{IR}}$  channels, was then added to the bath to distinguish  $\text{K}_{\text{IR}}$  activity from whole-cell currents. Currents were recorded on an Axopatch 200B amplifier (Molecular Devices), with signals filtered at 1 kHz and digitized at 5 kHz. Data were extracted and analysed using Clampfit 10.3 software (Molecular Devices). Cell capacitance ranged from 10 to  $16.5 \text{ pF}$  as measured by the amplifier. A 1M NaCl-agar salt bridge was added between the reference electrode and bath solution to minimize offset potentials. Experiments were performed at room temperature ( $21^\circ\text{C}$ ).

### Immunofluorescence

Isolated cerebral arterial SMCs from non-induced Cre SMC control and SMC  $\text{K}_{\text{IR}2.1}^{-/-}$  mice were probed for  $\text{K}_{\text{IR}2.1}$  and  $\text{K}_{\text{IR}2.2}$  protein expression. Cells were settled onto poly-L-lysine-treated cover glass and fixed in 4% paraformaldehyde (15 min,  $21^\circ\text{C}$ ). Fixed cells were then washed 3 times with PBS prior to permeabilization with 0.2% Tween 20 (15 min,  $21^\circ\text{C}$ ). A quench solution containing 0.2% Tween 20 and 3% donkey serum was used to block cells for one hour ( $21^\circ\text{C}$ ). Rabbit polyclonal primary antibodies against  $\text{K}_{\text{IR}2.1}$  (APC-026, 1:200; Alomone) and  $\text{K}_{\text{IR}2.2}$  (APC-042, 1:200; Alomone) were diluted in quench solution and

applied to cells for overnight incubation ( $4^\circ\text{C}$ ). The next day, cells were washed with 0.2% Tween 20 and treated with Alexa Fluor® 488 donkey anti-rabbit IgG (A-21206, 1:1000; ThermoFisher Scientific) fluorophore-conjugated secondary antibodies (1 hour,  $21^\circ\text{C}$ ). After additional washes, cells were mounted on slides with ProLong™ Diamond Antifade Mountant (ThermoFisher Scientific) with DAPI. Images were captured using a Leica-TCS SP8 confocal microscope (Wetzlar) with a  $63\times$  oil-immersion lens. Laser intensity was increased to visualize  $\text{K}_{\text{IR}2.1}$  staining as it exhibited a weak fluorescent signal. Controls for each stain were prepared by omitting the primary antibody. Mean fluorescence of each cell was measured using Image-J and background signal was subtracted using secondary antibody controls. We previously validated the specificity of anti- $\text{K}_{\text{IR}2.1}$  and anti- $\text{K}_{\text{IR}2.2}$  by pre-incubation with their corresponding blocking peptide antigen before addition to cells.<sup>15</sup> SMCs from mesenteric arteries were also used as  $\text{K}_{\text{IR}2.x}$  negative controls for these antibodies.<sup>15</sup>

### Western blot analysis

Isolated cerebral arteries were manually ground in ice-cold lysis buffer ( $150 \mu\text{L}$ ; Tissue Protein Extraction Reagent, ThermoFisher Scientific) with protease inhibitors (Protease Inhibitor Cocktail, Sigma-Aldrich). The supernatant was assayed for total protein using Pierce BCA Protein Assay (ThermoFisher Scientific). The samples were boiled for 10 min in Laemmli buffer containing 65 mM Tris HCL, 10% glycerol, 3% SDS, 0.6 mM Bromophenol blue and 2.5% 2-mercaptoethanol. Approximately  $1 \mu\text{g}$  of protein was loaded into an SDS-PAGE gel with a 4% to 10% gradient and run for 1.5 hrs at 100 V at  $21^\circ\text{C}$  (Bio-Rad). The gel was soaked in transfer buffer, set on a nitrocellulose membrane and left running at 25 V overnight at  $4^\circ\text{C}$ . The membrane was blocked with 5% non-fat dairy milk in Tris-buffered 0.1% Tween 20 (TBS-T) saline for 1 hr. After washing in 0.1% TBS-T, the membrane was incubated with rabbit polyclonal anti- $\text{K}_{\text{IR}2.2}$  (APC-042, 1:400; Alomone) in 1% milk TBS-T for 2 hrs at  $21^\circ\text{C}$ . After a TBS-T wash, the membrane was incubated with goat polyclonal anti-rabbit horseradish peroxidase-conjugated secondary antibodies (65-6120, 1:10000; ThermoFisher Scientific) in 1% milk TBS-T for 1 hr at  $21^\circ\text{C}$ . For standard controls, membranes were incubated with anti-pan actin rabbit polyclonal antibody (AAN01, 1:1000; Cytoskeleton Inc.) in 1% milk TBS-T for 2 hrs at  $21^\circ\text{C}$ . After washing, the blot was developed using Amersham ECL Prime Western Blotting Reagent (Cytiva, Global Life Sciences Solutions) and imaged on a Bio-Rad ChemiDoc™ MP Imaging System. Densitometric analysis was

performed using Image Lab 6.1 (Bio-Rad). Protein signal was normalized to actin levels.

### Cerebral vessel myography

Cerebral arteries were cannulated in a custom mounting chamber filled with physiological salt solution (PSS) containing (in mM): 119 NaCl, 4.7 KCl, 20 NaHCO<sub>3</sub>, 1.7 KH<sub>2</sub>PO<sub>4</sub>, 1.2 MgSO<sub>4</sub>, 1.6 CaCl<sub>2</sub>, and 10 glucose. Vessels were filled with Ca<sup>2+</sup>-PSS and an air bubble was passed from the cannula to strip the vessel of functional endothelium. Bath solution was continuously bubbled with air and maintained at 36.0 ± 0.2°C. Following equilibration at 15 mmHg for 30 min, 60 mM K<sup>+</sup> was superfused to assess vessel viability and measure minimum diameter. Absence of intact endothelium was confirmed by exposure to bradykinin (10 μM; Sigma Aldrich). After washing with Ca<sup>2+</sup>-PSS, the internal pressure of the vessel was adjusted to 20 mmHg and then increased stepwise to 100 mmHg in increments of 20 mmHg with 5 min per step. At 100 mmHg, bath K<sup>+</sup> was increased from 5 mM to 10 mM for approximately 1 min to assess K<sup>+</sup>-induced dilation. After excess K<sup>+</sup> was washed off, pressure was reduced to 20 mmHg and 100 μM Ba<sup>2+</sup> was added to the superfusate. The pressure challenge was repeated and, after recording the response at 100 mmHg, vessels were reassessed for K<sup>+</sup>-induced dilation. In a separate group of control animals, dilation to 10 mM K<sup>+</sup> was assessed before and after addition of 1 μM, 3 μM and 10 μM Ba<sup>2+</sup>. Passive vessel diameter was measured while repeating pressure steps in the presence of 2 mM EGTA in Ca<sup>2+</sup>-free PSS. The diameter was measured using an automated edge detection system (IonOptix) under a 10× objective on a Zeiss Axiovert 200 microscope (Carl Zeiss).

### Arterial spin-labeling magnetic resonance imaging of the brain

Under 2.2% isoflurane anesthesia, a polyethylene catheter (PE10; Instech Laboratories) was implanted intraperitoneally and connected to a syringe containing 1 mM phenylephrine. The animal was placed in a custom-built insert in the prone position and inserted in an Agilent Animal MRI scanner with a 9.4-Tesla, 31-cm horizontal bore magnet (Magnex Scientific), 60-mm gradient coil set of 1000 mT/m strength (Agilent), and Bruker Avance MRI III console with Paravision-6 software (Bruker BioSpin Corp). A 40-mm millipede volume coil (Agilent) was used for data acquisition.

An anatomical reference scan was acquired using a 2D fast spin echo (Turbo-Rapid Acquisition with Relaxation Enhancement (RARE)) sequence with the

following parameters: field of view (FOV) = 19.2 × 19.2 mm<sup>2</sup>, matrix size = 128 × 128, 11 slices with slice thickness of 1 mm, repetition time = 5000 ms, echo time (TE) = 10 ms, effective echo time = 40 ms, RARE factor = 8, number of averages = 1.

A flow-sensitive alternating inversion-recovery spin echo planar imaging sequence with a 180° hyperbolic secant radiofrequency inversion pulse was used (imaging parameters: TE = 17 ms; 5 slices with imaging slice thickness of 2 mm; image matrix = 64 × 50; FOV = 19.2 × 15 mm<sup>2</sup>, inversion parameters: inversion slab thickness = 13 mm; pulse length = 3 ms) for perfusion images. Eleven images with increasing inversion times (100 ms + *i* 300 ms (*i* = 0, 2, 3, ..., 10)) were obtained for each slice to determine T<sub>1</sub>. Images with slice selective inversion were acquired followed by images with nonselective inversion. From these images, T<sub>1sel</sub> and T<sub>1nonselect</sub> were calculated using a non-linear least square fit (ASL-Perfusion Processing; Bruker). The five 2-mm slices spanned the mouse brain with a total scan time of approximately 13 min.

During acquisition, the animal was maintained at ~1.75% isoflurane and breath rate was monitored (PC-SAM model #1025; SA Instruments, Inc.) with a pneumatic pillow. Body temperature was measured with a rectal probe and maintained at ~37°C with a homeothermic warm air blower. Mean arterial pressure (MAP) was measured with a tail cuff (CODA™ Monitor, Kent Scientific) during MRI acquisition. After a baseline scan of the brain was acquired, phenylephrine hydrochloride (0.816 mg kg<sup>-1</sup>; Sigma-Aldrich) was injected and the scan was repeated. Following completion of MRI, mice were euthanized via cervical dislocation under deep anesthesia. CBF (mL/100 g/min) was quantified in the cortex, cerebral nuclei, hippocampus, thalamus, hypothalamus and midbrain using custom software written in MATLAB (Mathworks, Inc.).

### Animal preparation for superior epigastric artery isolation

All experiments were approved and conducted in accordance with the guidelines set by the Institutional Animal Care and Use Committees at the University of Vermont and Michigan State University. Superior epigastric arteries (SEAs) were isolated from euthanized C57BL/6 (control) and tamoxifen-inducible SMC-specific K<sub>IR2.1</sub> knockout (SMC K<sub>IR2.1</sub><sup>-/-</sup>) mice as described.<sup>22-24</sup> For administration of tamoxifen, 6-week-old SMC K<sub>IR2.1</sub><sup>-/-</sup> mice were anesthetized with isoflurane (3% in O<sub>2</sub>), and the interscapular area was shaved and sterilized. A small, subcutaneous pocket was made with blunt dissection and tamoxifen citrate extended-release pellets (5 mg total with 21-day

release; Innovative Research of America) were implanted, followed by wound closure. Animals were euthanized a minimum of 4 weeks after pellet implantation for tissue collection.

### Electrophysiology and qRT-PCR

SEAs were enzymatically dissociated to yield single SMCs for perforated-patch recording of  $Ba^{2+}$ -sensitive  $K^+$  currents to quantify the functional expression of SMC  $K_{IR}$  channels, and for qRT-PCR as described.<sup>22–24</sup> For detailed description of electrophysiology, see supplemental material. Briefly, settled SMCs in the recording chamber were superfused with PSS. Pipettes were applied to the cell surface and after electrical access to cytoplasm was attained, cells were superfused with PSS containing 60 mM  $K^+$ . Cells were then held at  $-50$  mV and subjected to 200 ms voltage ramps from  $-120$  mV to  $+20$  mV in the absence or presence of  $Ba^{2+}$  (100  $\mu$ M). Currents were normalized to cell capacitance.

Samples were prepared using a modified isolation protocol for single-cell qRT-PCR, as described.<sup>25,26</sup> Briefly, SEA SMCs were enzymatically isolated, and samples of  $\sim 50$  cells were aspirated into glass micropipettes filled with RNA isolation buffer for use in Ambion® Single Cell-to-CT qRT-PCR kit (ThermoFisher Scientific). Reactions were then prepared using TaqMan gene expression MasterMix (ThermoFisher Scientific) and primers for  $K_{IR2.1}$  (*Kcnj2*; RefSeq NM\_008425.4),  $K_{IR2.2}$  (*Kcnj12*; RefSeq NM\_001267593.1) and smooth muscle  $\alpha$ -actin (*Acta2*; RefSeq NM\_007392.3) (ThermoFisher Scientific). Transcripts were preamplified for 14 cycles prior to qRT-PCR, as per manufacturer's instructions. Quantitative RT-PCR for the transcripts of interest was then run for 40 cycles. No-template controls were included throughout. Sample mRNA expression of *Kcnj2* and *Kcnj12* were normalized to *Acta2* expression as described.<sup>25</sup>

### Superior epigastric vessel myography

SEAs were cannulated onto glass micropipettes and studied by pressure myography as described.<sup>22–24</sup> Vessels were warmed to  $37^\circ\text{C}$ , pressurized to 80 cm  $H_2O$  and allowed to develop myogenic tone or were pre-constricted with phenylephrine if myogenic tone was less than 10% ( $10^{-6}$  M). The cannulated arteries were superfused with PSS (5 mM  $K^+$ ), or solutions containing 8 mM or 15 mM  $K^+$  (KCl substituted for NaCl in PSS) in the absence or presence of  $Ba^{2+}$  (100  $\mu$ M).

### Statistical analysis

Data were analyzed using GraphPad Prism 8 (GraphPad Software) and are expressed as

mean  $\pm$  SD. Distribution was determined with Shapiro-Wilk test.  $P < 0.05$  was considered statistically significant.

## Results

### *K<sub>IR</sub>* currents persist despite *K<sub>IR2.1</sub>* ablation in smooth muscle cells of cerebral arteries

In cerebral arterial smooth muscle,  $K_{IR2.1}$  subunits are presumed to be the dominant isoform driving the native  $K_{IR2.x}$  current.<sup>10</sup> To explore this concept, initial experiments sought to delineate the impact of  $K_{IR2.1}$  knockout on whole-cell  $Ba^{2+}$ -sensitive inwardly rectifying  $K^+$  currents in freshly isolated SMCs. Figure 1 denotes the presence of a robust inward current in both tamoxifen-induced SMC *K<sub>IR2.1</sub><sup>-/-</sup>* and non-induced control animals (Cre recombinase carriers with floxed  $K_{IR2.1}$  gene). The observed currents were readily activated by extracellular  $K^+$  and blocked by micromolar  $Ba^{2+}$ , signature characteristics of vascular  $K_{IR2.x}$  channels. On aggregate,  $Ba^{2+}$ -sensitive currents were modestly reduced in SMC *K<sub>IR2.1</sub><sup>-/-</sup>* mice ( $5.83 \pm 1.88$  pA/pF) compared to controls ( $7.12 \pm 2.63$  pA/pF), but this difference was not statistically significant (Figure 1(c)). This absence of  $K_{IR}$  current knockdown was also observed in SMCs isolated from superior epigastric arteries (SEAs) of SMC *K<sub>IR2.1</sub><sup>-/-</sup>* mice (Figure S2(a,b)). To verify that Cre SMC control mice do not have reduced  $K_{IR}$  current potentially resulting from leaky Cre recombinase activity,  $Ba^{2+}$ -sensitive  $K^+$  currents were measured in cerebral SMCs of C57BL/6 mice. We found no difference between non-induced Cre SMC control and C57BL/6 control animals ( $7.12 \pm 2.63$  pA/pF vs.  $6.88 \pm 1.67$  pA/pF respectively,  $P = 0.85$ , unpaired *t*-test).

### *K<sub>IR2.1</sub>* expression was reduced post-knockout in cerebral arterial smooth muscle cells without impact on *K<sub>IR2.2</sub>*

The whole-cell currents we observed, while indicative of strong rectifying  $K_{IR2.x}$  activity, likely exist as a composite of all  $K_{IR2.x}$  channels expressed in VSM. Therefore, to further discern the contributions of individual  $K_{IR2.x}$  subunits, we screened for subunits commonly described in cerebral arterial smooth muscle— $K_{IR2.1}$  and  $K_{IR2.2}$ .<sup>15</sup> Immunostaining of  $K_{IR2.1}$  revealed a diffuse expression pattern (Figure 2(a)). Mean global cell fluorescence of  $K_{IR2.1}$  antibody signal was reduced in SMC *K<sub>IR2.1</sub><sup>-/-</sup>* mice when compared with the control group (Figure 2(b)). In contrast,  $K_{IR2.2}$  was predominantly concentrated at the plasma membrane (Figure 2(c)) and the induction of  $K_{IR2.1}$  deletion did not impact the expression of  $K_{IR2.2}$

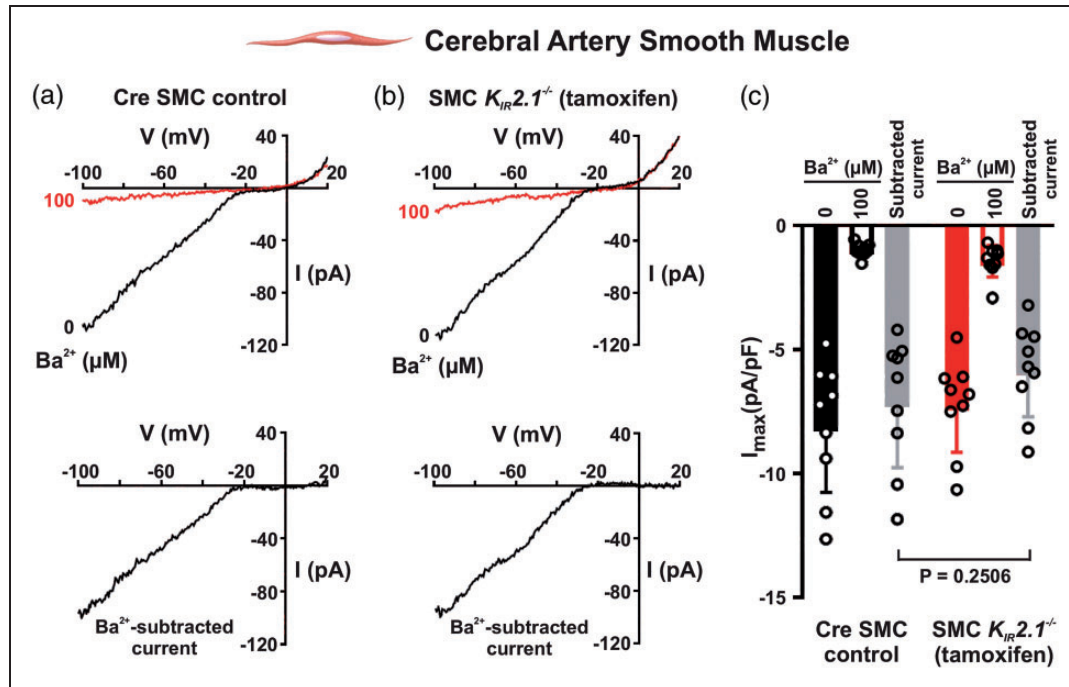


**Figure 1.** Genetic ablation of  $K_{IR2.1}$  does not eliminate inward  $K^+$  currents in cerebral arterial smooth muscle cells (SMCs). Whole-cell patch clamp electrophysiology was used to measure  $K_{IR}$  current with voltage ramps from  $-100$  to  $+20$  mV in the absence and presence of  $Ba^{2+}$  in  $60$  mM  $K^+$ . (a,b) Representative recordings of whole-cell and  $Ba^{2+}$ -subtracted  $K_{IR}$  currents in myocytes isolated from SMC  $K_{IR2.1}^{-/-}$  mice and non-induced Cre SMC controls. (c) Summary data compare peak inward current at  $-100$  mV between groups ( $n = 9$  SMCs from 6 mice in control group and  $n = 9$  SMCs from 8 mice in knockout group; nested  $t$ -test).

(Figure 2(d)). To further confirm that SMC  $K_{IR2.1}$  deletion does not lead to compensatory changes in  $K_{IR2.2}$  expression, western blot analysis was performed for  $K_{IR2.2}$ . Since  $K_{IR2.2}$  is expected to be expressed in SMCs and not endothelial cells (ECs), intact cerebral arteries were used. Indeed, protein levels of  $K_{IR2.2}$  were similar in control and SMC  $K_{IR2.1}^{-/-}$  mice (Figure 3).

While contrary to initial reports,<sup>10,17</sup> the expression pattern in our study aligns with more recent molecular work highlighting  $K_{IR2.2}$  dominance over  $K_{IR2.1}$  at the mRNA level in mouse cerebral arterial SMCs (Figure 4). Furthermore, Q-PCR assessments performed on SMCs from SEAs revealed a comparable expression pattern, with  $K_{IR2.2}$  dominating over  $K_{IR2.1}$  (Figure S2(c)).

### Myogenic responses and $K^+$ -induced dilation are maintained in cerebral arteries of SMC $K_{IR2.1}^{-/-}$ mice

$K_{IR}$  channels maintain resistance arteries in a hyperpolarized state at low pressure and their activity diminishes as vessels develop tone at higher pressure.<sup>15</sup> We examined the impact of SMC  $K_{IR2.1}$  deletion on myogenic tone development in endothelium-denuded cerebral arteries. Lack of dilatory response to bradykinin

confirmed successful disruption of endothelium;  $144 \pm 16 \mu\text{m}$  vs.  $144 \pm 15 \mu\text{m}$  diameter before and after application of bradykinin, respectively,  $n = 11$ . As control arteries were pressurized from 20–100 mmHg, a strong pressure-induced constriction was observed, a response that was comparable to vessels isolated from tamoxifen-induced mice (not statistically significant based on an unpaired  $t$ -test; Figure 5(a) and (b)). To discern  $K_{IR}$  activity,  $Ba^{2+}$  was added to bath solution. At low pressures (20–40 mmHg), where vessels are hyperpolarized with low myogenic tone,  $Ba^{2+}$  treatment induced constriction (Figure 5(b)). As pressure was elevated and vessels depolarized, the effects of  $Ba^{2+}$  became attenuated. This response pattern was comparable between the two groups, indicating that  $K_{IR}$  contributions to the functional phenotype of the de-endothelialized vessels were intact despite SMC-specific  $K_{IR2.1}$  deletion. Increasing extracellular  $K^+$  potentiates  $K_{IR}$  channels, promoting membrane hyperpolarization and vessel dilation.<sup>27</sup> Bath  $K^+$  was increased from 5 mM to 10 mM and dilatory responses attributed to  $K_{IR}$  were measured before and after treatment with 100- $\mu\text{M}$   $Ba^{2+}$ . This experiment further confirmed that SMC  $K_{IR2.1}$  knockout had no significant functional effect as  $K^+$ -induced dilation was present in SMC  $K_{IR2.1}^{-/-}$  vessels and was abrogated after treatment with 100- $\mu\text{M}$   $Ba^{2+}$  in both groups (Figure 5(c)).

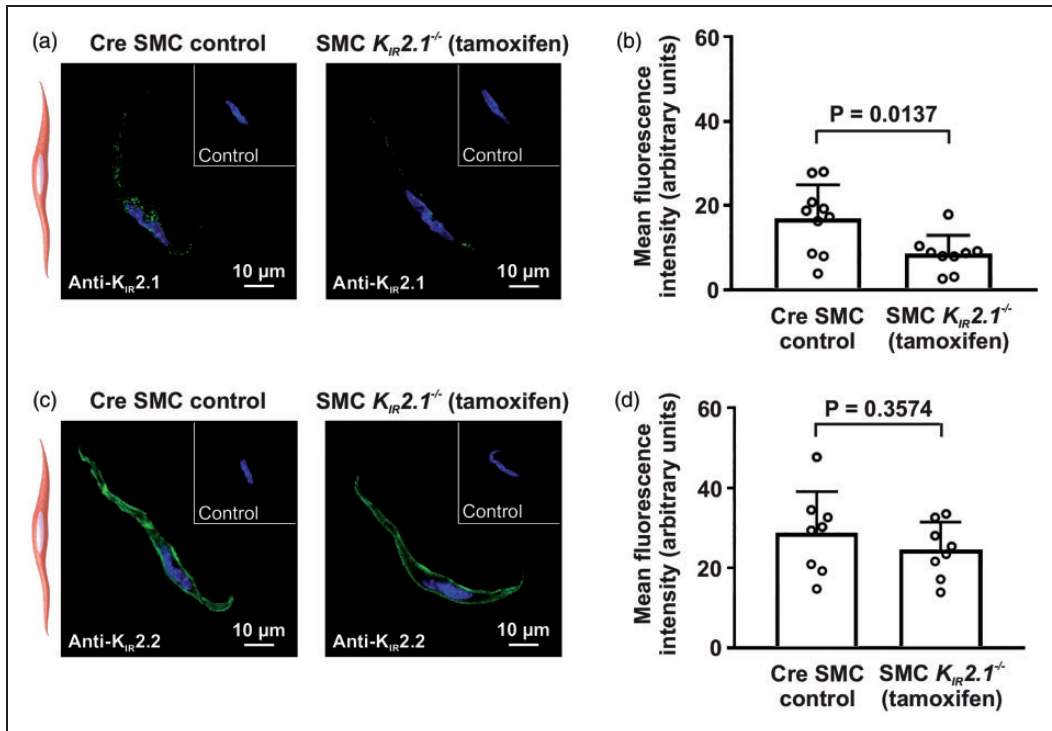


**Figure 2.**  $K_{IR}2.1$  is negligibly expressed in cerebral vascular smooth muscle cells (SMCs) while  $K_{IR}2.2$  is highly expressed at the cell membrane. Tamoxifen-induced  $K_{IR}2.1$  knockout significantly reduced subunit expression but levels remained detectable by immunofluorescence. (a) Fluorescent anti- $K_{IR}2.1$  (green) exhibited a faint labeling pattern in cerebral arterial myocytes from SMC  $K_{IR}2.1^{-/-}$  and control mice with nuclei stained with DAPI (blue). (b) Summary of data compares fluorescence intensity (background subtracted) of  $K_{IR}2.1$  signal between groups ( $n = 10$  cells from 5 animals in control group and  $n = 9$  cells from 5 animals in knockout group; unpaired *t*-test). (c) Immunofluorescence labeling of SMCs for  $K_{IR}2.2$ . (d) Summary of data compares background-subtracted fluorescence intensity of  $K_{IR}2.2$  signal between groups ( $n = 8$  cells pooled from 4 animals/group; unpaired *t*-test). Two cells were analyzed per animal with background signal subtracted using 2° antibody control.

Specifically,  $Ba^{2+}$ -sensitive,  $K^+$ -induced vasodilation was  $5.5 \pm 3.9\%$  in control vessels and  $4.0 \pm 2.3\%$  in vessels from SMC  $K_{IR}2.1^{-/-}$  mice. Intriguingly, this response was also significantly blocked at low  $Ba^{2+}$  concentrations ( $3 \mu M$ ; Figure 5(d)), a finding more consistent with the  $Ba^{2+}$  sensitivity profile of  $K_{IR}2.2$ .<sup>16</sup> We also examined dilatory responses in pressurized SEAs and found that  $Ba^{2+}$ -sensitive,  $K^+$ -induced vasodilation was comparable between the two groups (Figure S2(e)).

#### Region-specific brain perfusion is maintained in SMC $K_{IR}2.1^{-/-}$ mice

Functional hyperemia in the brain, often termed neurovascular coupling, has been linked to the activation of SMC  $K_{IR}$  by extracellular  $K^+$ .<sup>28</sup> These channels have also been implicated in cerebral autoregulation as they respond to changes in intravascular pressure.<sup>15</sup> Considering these functions, we assessed the effects of SMC-specific  $K_{IR}2.1$  knockout on cerebral perfusion at rest and in response to a systemic blood pressure challenge. Animals were instrumented and placed in

an MRI scanner for blood flow measurement by ASL before and after intraperitoneal phenylephrine injection. At rest, there were no significant differences between control and SMC  $K_{IR}2.1^{-/-}$  mice in perfusion of the cortex, cerebral nuclei, hippocampus, thalamus, hypothalamus, and midbrain (Figure 6). Phenylephrine injection increased MAP from  $99 \pm 16$  mmHg to  $109 \pm 17$  mmHg ( $P < 0.05$ ), as measured via tail cuff. Of note, MAP did not differ between the two groups of mice and so results were pooled. The phenylephrine treatment resulted in a small but significant rise in CBF in all the brain regions analyzed (Figure 6). However, the magnitude of this response did not differ between the two groups (Figure 6(b)).

#### Knockout of SMC $K_{IR}2.1$ has no significant effect on $Ba^{2+}$ -sensitive currents and $K^+$ -induced dilation of superior epigastric arteries

In SEAs, tamoxifen-inducible knockout of SMC  $K_{IR}2.1$  had no significant effect on  $Ba^{2+}$ -sensitive currents compared to control C57BL/6 mice (Figure S2(a, b)). In fact, mRNA analysis indicated that  $K_{IR}2.2$

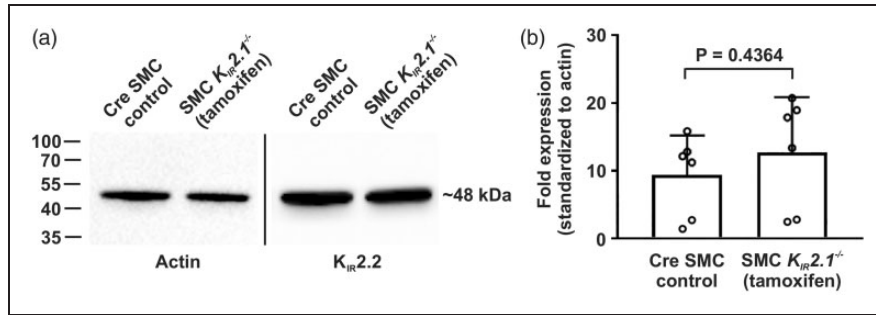


**Figure 3.**  $K_{IR}2.2$  protein expression is unaltered in smooth muscle cell (SMC)  $K_{IR}2.1^{-/-}$  cerebral arteries. (a) Western blot of intact cerebral arteries confirmed that protein levels of  $K_{IR}2.2$  are not impacted by deletion of SMC  $K_{IR}2.1$ . (b) Summary of data compares  $K_{IR}2.2$  protein levels between control and knockout mice (normalized to actin;  $n = 6$  mice; unpaired  $t$ -test).

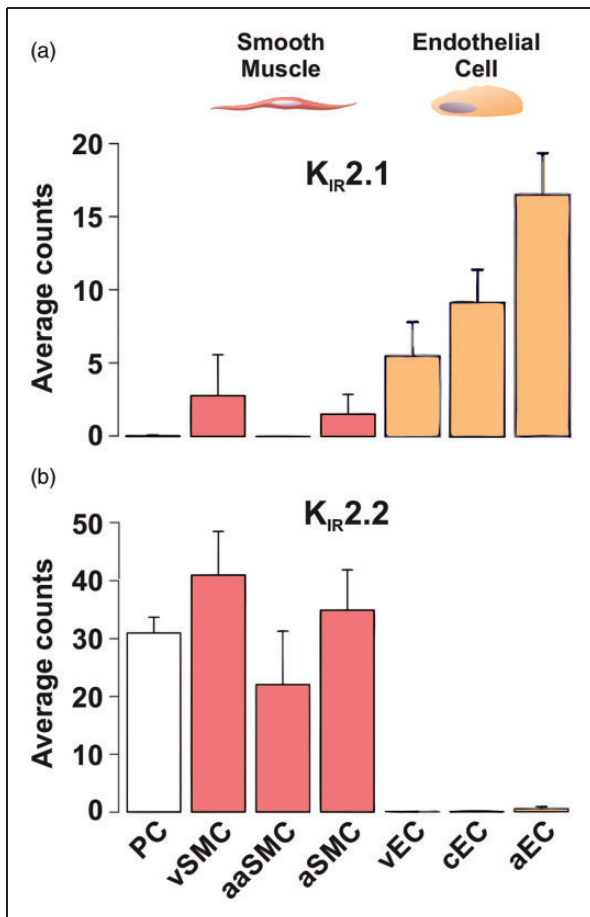


**Figure 4.**  $K_{IR}2.1$  and  $K_{IR}2.2$  subunits are inversely expressed in cerebral endothelial and vascular smooth muscle cells. (a)  $K_{IR}2.1$  and (b)  $K_{IR}2.2$  subunit expression is shown as average cellular transcript counts per cell, as determined by single-cell RNA sequencing of the mouse brain vasculature. Data highlight differences in the dominant subunit between cell types. Abbreviations: PC – pericytes; SMC – smooth muscle cells; EC – endothelial cells; v – venous; c – capillary; a – arterial; aa – arteriolar. Figures provided by <http://betsholtzlab.org/VascularSingleCells/database.html>.<sup>33,34</sup>

expression dominates  $K_{IR}2.1$  expression in epigastric artery SMCs of SMC  $K_{IR}2.1^{-/-}$  mice (Figure S2(c)) and C57BL/6 control mice, as we previously showed.<sup>23</sup> We also examined myogenic tone in these vessels under pressure (Figure S2(d)). While  $Ba^{2+}$ -induced constriction in 5 mM  $K^+$  PSS was similar in C57BL/6 ( $20 \pm 3.4\%$  constriction,  $n = 5$ ) and SMC  $K_{IR}2.1^{-/-}$  mice ( $17 \pm 18\%$  constriction,  $n = 8$ ;  $P = 0.7241$ ; Mann-Whitney U-test), myogenic tone at 80 cm  $H_2O$  was significantly increased in the knockout with considerable variability. Elevated extracellular  $K^+$  dilated SEAs from C57BL/6 mice in a concentration-dependent manner and  $Ba^{2+}$  (100  $\mu M$ ) inhibited this response, implicating  $K_{IR}$  channels in the mechanism of action (Figure S2(e)). Knockout of SMC  $K_{IR}2.1$  had no effect on the magnitude of this dilatory response.

## Discussion

This study explored the role that  $K_{IR}2.1$  plays within the cerebral vasculature using an inducible, SMC-specific genetic ablation model. The persistence of  $Ba^{2+}$ -sensitive  $K^+$  currents following deletion of  $K_{IR}2.1$  raised the possibility that other subunits underlie the smooth muscle inward  $K^+$  conductance. Functional experiments reinforced this idea as reduced SMC expression of  $K_{IR}2.1$  did not markedly impact myogenic reactivity of cerebral arteries and maintenance of blood flow to various brain regions. The high expression of  $K_{IR}2.2$  subunits, as detected by immunofluorescence and RNA sequencing in myocytes, may account for this minimal functional impact. The lack of phenotype following  $K_{IR}2.1$  knockout was mirrored in experiments conducted in SEAs, indicating that these observations are not limited to the cerebral vasculature. These findings highlight that arterial responses are not dependent on  $K_{IR}2.1$

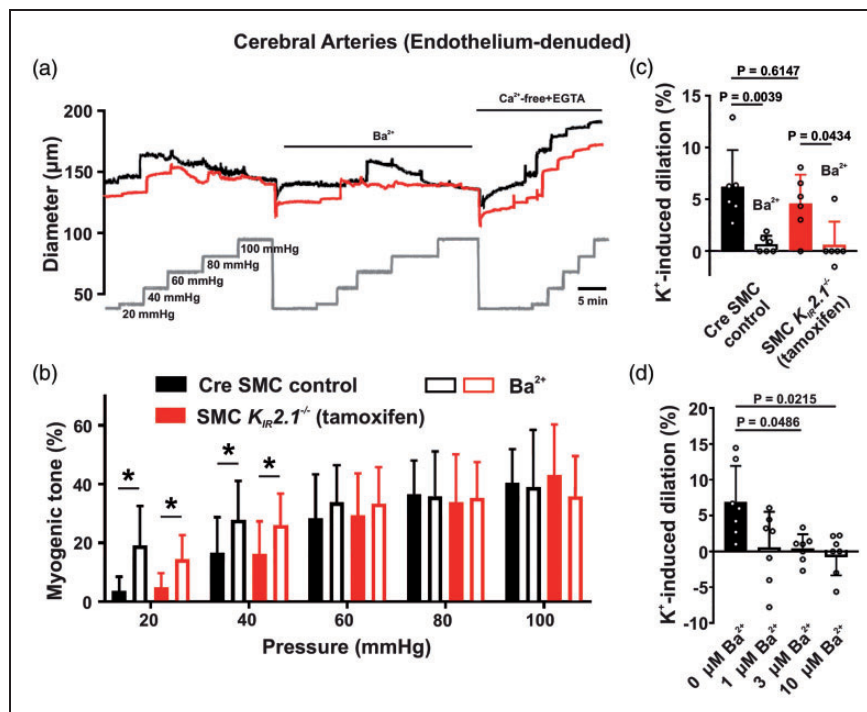


**Figure 5.** Myogenic responses and K<sup>+</sup>-induced dilation are intact in cerebral arteries of smooth muscle cell (SMC) *K<sub>IR2.1</sub><sup>-/-</sup>* mice. Cerebral arteries from control and SMC *K<sub>IR2.1</sub><sup>-/-</sup>* mice were cannulated and intravascular pressure was elevated stepwise while vasomotor responses were measured. (a) Representative diameter traces from endothelium-denuded vessels of control and SMC *K<sub>IR2.1</sub><sup>-/-</sup>* mice show the effect of increasing pressure on myogenic tone. (b) Summary of data highlights limited impact of smooth muscle *K<sub>IR2.1</sub>* knockout on myogenic tone development. Paired *t*-test was performed for 0 vs. 100 µM Ba<sup>2+</sup> treatment ( $n = 10$  vessels in the control group and  $n = 11$  vessels in the SMC *K<sub>IR2.1</sub><sup>-/-</sup>* group with 1 vessel/mouse; \* $P < 0.05$ ). (c) K<sup>+</sup>-induced dilation, elicited by increasing extracellular K<sup>+</sup> from 5 mM to 10 mM before and after treatment with 100-µM Ba<sup>2+</sup>, was intact in the knockout group ( $n = 6$  vessels in the control group and SMC *K<sub>IR2.1</sub><sup>-/-</sup>* group; one-way ANOVA with Sidak's multiple comparisons test). (d) K<sup>+</sup>-induced dilation (5 mM K<sup>+</sup> to 10 mM K<sup>+</sup>) was abrogated with exposure to low concentrations of Ba<sup>2+</sup>, implicating *K<sub>IR2.2</sub>* as the mediator of this response based on its Ba<sup>2+</sup> sensitivity profile ( $n = 7$  vessels from control mice; repeated measures one-way ANOVA with Sidak's multiple comparisons test). Myogenic tone (%) was calculated as: [(passive diameter – active diameter)/(passive diameter – minimal diameter)] × 100 at each pressure step. K<sup>+</sup>-induced dilation (%) was calculated as difference between diameter at 10 mM [K<sup>+</sup>] and 5 mM [K<sup>+</sup>] divided by the dilatatory range (passive diameter – minimal diameter).

expression in SMCs and suggest the involvement of a more diverse pool of *K<sub>IR</sub>* subunits.

Contractility of the VSM layer is tightly coupled to intracellular Ca<sup>2+</sup> sourced through VGCCs, thereby creating a close relationship between  $V_M$  and diameter.<sup>7</sup> K<sup>+</sup> channels regulate the influx of Ca<sup>2+</sup> by hyperpolarizing  $V_M$  to promote relaxation and vasodilation.<sup>8</sup> The strong-rectifying *K<sub>IR2.x</sub>* family of channels are especially prominent within cerebral vessels where they are active under basal conditions to hyperpolarize  $V_M$ .<sup>8,15,29</sup> Although their role appears subtle, altering *K<sub>IR</sub>* activity translates to significant effects on vessel diameter and reactivity. *K<sub>IR</sub>* channel inhibition with Ba<sup>2+</sup> causes vasoconstriction, reduces flow, and prevents K<sup>+</sup>-induced dilation in rat cerebral and human brachial arteries.<sup>3,14,30</sup> Furthermore, *K<sub>IR</sub>* channels amplify other dilatatory responses through their intrinsic property of negative slope conductance.<sup>19,29,31</sup> They are also modulated by hemodynamic forces, specifically

intravascular pressure and flow.<sup>14,15</sup> Given their pleiotropic roles, it is logical to expect that knockout would generate a robust physiological phenotype.

This study began by examining native *K<sub>IR</sub>* currents in vascular smooth muscle isolated from cerebral arteries. To our surprise, comparable *K<sub>IR</sub>* activity was detected in SMC *K<sub>IR2.1</sub><sup>-/-</sup>* and control mice. While currents trended slightly lower in the knockout animals, no significant difference was observed between the two groups. These findings suggest the predominance of another *K<sub>IR</sub>* subunit—one with similar electrophysiological properties. Based on Ba<sup>2+</sup> sensitivity and unitary conductance, *K<sub>IR2.2</sub>* is a logical target and it should be noted that this subunit can heteromultimerize with *K<sub>IR2.1</sub>*.<sup>16,32</sup> With this in mind, we sought to observe the localization of key *K<sub>IR</sub>* subunits in cerebral arterial SMCs. Antibodies revealed a punctate labeling pattern for *K<sub>IR2.1</sub>* that was weak in control mice and was further diminished after

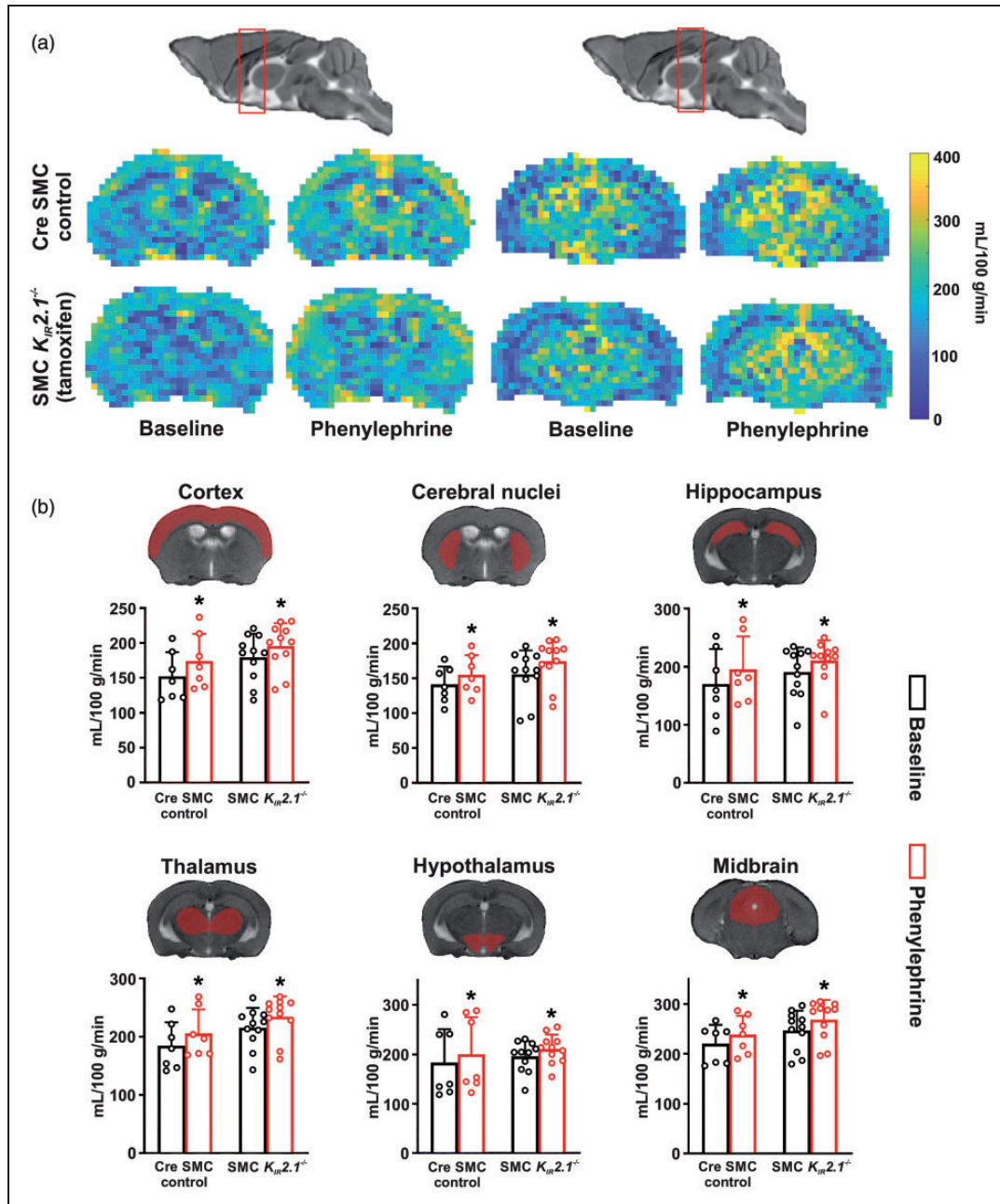


**Figure 6.** Region-specific brain perfusion is not altered in smooth muscle cell (SMC)  $K_{IR2.1}^{-/-}$  mice at rest and with increased systemic blood pressure. (a) Representative arterial spin-labeled MR brain perfusion maps. Scans were done in a posterior-to-anterior direction and the volume of brain scanned was divided into 5 coronal slices. Resting cerebral blood flow was measured in control and SMC  $K_{IR2.1}^{-/-}$  mice. Scans were repeated after blood pressure challenge with an intraperitoneal phenylephrine injection. Figure shows slices from 2 regions of the brain (red boxes) spanning cerebral nuclei, hippocampus, thalamus, and hypothalamus. (b) Baseline perfusion in several major brain structures was not significantly different between control and tamoxifen-induced mice. The blood pressure challenge caused a modest but significant rise in cerebral blood flow to a similar extent in control and SMC  $K_{IR2.1}^{-/-}$  animals. Unpaired t-test was performed for control ( $n = 7$  mice) vs. SMC  $K_{IR2.1}^{-/-}$  ( $n = 11$  mice) comparison; paired t-test was performed for baseline vs. phenylephrine-treatment. \* $P < 0.05$  compared to baseline control.

tamoxifen-induced conditional deletion. As to other pertinent  $K_{IR}$  subunits, we found that  $K_{IR2.2}$  is abundantly concentrated at the SMC plasma membrane. While these results contradict the historical view of

$K_{IR2.1}$  being the dominant subtype in cerebral SMCs, they do align with recent reports on single-cell RNA sequencing of cerebrovascular cells.<sup>33,34</sup> Specifically, this transcriptomic analysis revealed that

$K_{IR2.1}$ , while being highly expressed in ECs, was decidedly less abundant in arterial SMCs.<sup>33,34</sup> Conversely,  $K_{IR2.2}$  mRNA expression was markedly greater in SMCs but negligible in ECs. A similar pattern was reported in SMCs and ECs from SEAs.<sup>23</sup> This differential expression pattern, in concert with our functional data, reinforces the notion that expression of  $K_{IR2.1}$  in SMCs is not central to cerebral vessel function.

Elevation of extracellular  $K^+$  enhances  $K_{IR}$  channel activity and drives arterial dilation. This stimulus is thought to contribute to functional hyperemia in the brain.<sup>28</sup> In our SMC  $K_{IR2.1}^{-/-}$  mice,  $Ba^{2+}$ -sensitive  $K^+$ -induced dilation was conserved and equal in magnitude to control animals. Thus, while our data show this response is  $K_{IR}$  mediated, another subtype appears to be involved. Based on expression data,<sup>33,34</sup>  $K_{IR2.2}$  was viewed as the most likely subtype. The identity of  $K_{IR}$  subunits driving cell-specific  $K_{IR}$  currents can be differentiated based on their  $Ba^{2+}$  sensitivity;  $K_{IR2.1}$  and  $K_{IR2.2}$  both are blocked in the micromolar range but  $K_{IR2.2}$  is 10 times more sensitive.<sup>16,32</sup> Thus, we tested  $K^+$ -induced dilation in cerebral arteries of control mice before and after application of low concentrations of  $Ba^{2+}$  (1  $\mu$ M to 10  $\mu$ M) and found this response was abolished, consistent with  $K_{IR2.2}$  activity.

Our electrophysiology and myography results contrast work in a global  $K_{IR2.1}^{-/-}$  mouse,<sup>17</sup> where genetic deletion abolished inward  $K^+$  currents in cerebral SMCs and  $K^+$ -induced dilation. While seemingly at odds, it should be recognized that the global knockout displays severe developmental defects (cleft palate) and as death occurs within 24 hrs of birth, neonatal rather than adult vessels were used—a technically challenging prospect. This can be problematic as early postnatal SMCs may not be fully differentiated, differing in contractile phenotype compared to adult SMCs.<sup>35–37</sup> It should also be noted that  $K_{IR2.1}$  is functionally important in cerebral arterial ECs, and, as such, the functional phenotype changes observed in the global knockout may be influenced by the deletion in ECs.

Smooth muscle  $K_{IR}$  channels are sensitive to hemodynamic forces; as intraluminal pressure rises, their activity is suppressed whereas low pressure has the opposite effect.<sup>14,15</sup> This aligns with increased  $Ba^{2+}$  sensitivity—reflective of greater  $K_{IR}$  activity—of cerebral arteries at lower pressures.<sup>15</sup> Intriguingly, pressure sensitivity was reported to be modulated by cholesterol, with depletion increasing  $K_{IR}$  activity in SMCs, consistent with this lipid stabilizing  $K_{IR}$  channels in the closed state.<sup>15</sup> This finding translated into whole vessels, with increased  $Ba^{2+}$ -induced constriction being observed in denuded cerebral arteries at elevated pressure after cholesterol depletion.<sup>15</sup> This work helped define a new paradigm of hemodynamic sensing

coupled to specific  $K_{IR}$ -lipid interactions in the cerebral vasculature. Based on the pressure- $K_{IR}$  relationship, we expected mice deficient in smooth muscle  $K_{IR2.1}$  to exhibit diminished myogenic responses to pressure. Such an impairment would be expected to impact CBF regulation, manifesting as enhanced brain perfusion on ASL perfusion maps. Contrary to these expectations, we found that region-specific brain perfusion was comparable between SMC  $K_{IR2.1}^{-/-}$  mice and controls and did not differ among the two groups after a phenylephrine-induced systemic blood pressure challenge. This implies a limited role for SMC  $K_{IR2.1}$  in conferring pressure sensitivity in the cerebral vasculature. One limitation of our study is that CFB was not fully maintained at baseline after high dose phenylephrine, perhaps due to blunting of autoregulation by isoflurane.<sup>38</sup> Tail cuff measure of blood pressure accentuates this concern because it underestimates true in vivo readings.<sup>39</sup> As such, our phenylephrine challenge likely elicited a response greater than 10 mmHg, which also implies tone was not heavily impaired. Finally, it should be noted that complexity of the MRI setup precluded collection of end-tidal  $CO_2$  values during the scans, although we did actively monitor and maintain breath rate with small anesthetic flow adjustments.

$K_{IR}$  currents in ECs are markedly larger than those in SMCs.  $K_{IR2.1}$  is indispensable in ECs with a major role in endothelium-dependent dilation, particularly in amplifying the impact of other active vasodilatory  $K^+$  channels.<sup>19</sup> Endothelial  $K_{IR}$  channels are also tied to hemodynamic sensing, with shear stress potentiating the native cerebral arterial current. This potentiation facilitated flow-induced vasodilation and was dependent on interactions with phosphatidylinositol 4,5-bisphosphate.<sup>15</sup> The ability of lipids to regulate EC and SMC  $K_{IR}$  highlights the potential involvement of these channels in pathophysiological mechanisms in dyslipidemic disorders.

Based on our work, we believe that the observed differences between EC and SMC  $K_{IR}$  channel pools in hemodynamic and lipid sensitivity stem from differences in subunit composition. Subunit identity further becomes relevant when considering molecular interactions in mechanotransduction pathways potentially involving  $K_{IR2.x}$  subunits. Specifically,  $K_{IR2.1}$  and  $K_{IR2.2}$  differ in protein binding capability, which may in turn influence the formation of signalling complexes. Moreover, several members of the dystrophin-associated protein complex, which links the plasma membrane to the cytoskeleton, associate more strongly with the C-terminus of  $K_{IR2.2}$  as opposed to  $K_{IR2.1}$  where interactions are weak.<sup>40</sup> This disparity was attributed to differences in PDZ binding motifs and upstream amino acid sequences of these channels.

While the differences are intriguing, functional implications of these interactions remain unexplored.

We also examined the role of  $K_{IR}2.1$  in a skeletal muscle resistance artery—the superior epigastric artery.  $K_{IR}$  channels appear to contribute substantially to resting membrane potential and myogenic tone at normal blood pressure levels in SEAs.<sup>23</sup> We previously reported that SMCs in these arteries predominately express mRNA for  $K_{IR}2.2$  with little mRNA for  $K_{IR}2.1$  in C57BL/6 mice.<sup>23</sup> Consistent with these findings, we observed low abundance of  $K_{IR}2.1$  in superior epigastric myocytes from SMC  $K_{IR}2.1^{-/-}$  mice, whereas  $K_{IR}2.2$  expression was substantially higher and similar to reported levels for this arterial network.<sup>23</sup> SMC  $K_{IR}$  currents and  $Ba^{2+}$ -sensitive,  $K^{+}$ -induced dilation of isolated SEAs appeared unaffected by deletion of SMC  $K_{IR}2.1$ . This suggests, similar to cerebral vessels, SMC  $K_{IR}2.1$  does not play a major role. However, we did observe increased myogenic tone in isolated SEAs in our knockout, indicating that there may be some subtle effect of SMC  $K_{IR}2.1$  deletion in these vessels. The mechanism responsible for this elevated myogenic tone was not explored further. Nonetheless, all other measures of  $K_{IR}$  channel function, including  $K_{IR}$  currents,  $K^{+}$ -induced vasodilation, and  $Ba^{2+}$ -induced constriction, appeared unaffected by knockout of  $K_{IR}2.1$  in SMCs. These data lead us to conclude, that, like the cerebral vasculature, expression and function of  $K_{IR}2.1$  channels in SEA SMCs appears minimal, and other  $K_{IR}$  channels such as  $K_{IR}2.2$  may be more functionally relevant.

## Summary

Cerebral blood flow is a highly regulated process, where adjustments to perfusion occur in response to transient local stimuli and sustained hemodynamic forces. These adjustments ensure adequate nutrient delivery while preventing brain injury from hypo- or hypertension. This remarkable feat is intimately tied to a diverse collection of ion channels in ECs and SMCs whose composite actions regulate vascular tone. Expressed in both ECs and SMCs,  $K_{IR}$  channels participate in tone regulation through  $V_M$  establishment,  $K^{+}$  response amplification, and force sensing in cerebral arteries.<sup>3,15,19,29</sup> Historically,  $K_{IR}2.1$  was viewed as a major contributor to the inward  $K^{+}$  conductance in cerebral SMCs. Our observations lie in contrast, with  $K_{IR}$  activity persisting at the isolated cell, intact vessel, and live animal levels after SMC-specific  $K_{IR}2.1$  knockout. This minimal functional impact suggests that  $K_{IR}2.1$  is either a redundant component of the channel pool or its activity is minor relative to other  $K_{IR}$  subunits in VSM. Indeed, we found that  $K_{IR}2.1$  expression in SMCs is modest, while a

different subunit— $K_{IR}2.2$ —was found abundantly localized to the plasma membrane. To conclude, our work highlights that cerebral SMC  $K_{IR}$  responses are not dependent on  $K_{IR}2.1$  and suggests that the native channel pool is more heterogenous in composition than previously thought.

## Funding

The author(s) disclosed receipt of the following financial support for the research, authorship, and/or publication of this article: This work was funded by Canadian Institutes of Health Research (Project # RN354019) granted to DGW. WFJ was supported by National Institutes of Health (NIH) grants HL-137694 and PO1-HL-070687. NRT was supported by NIH grants DK119615 and K01-DK103840.

## Acknowledgements

We are grateful to Miranda Bellyou and Dr. Alex Li (Western University) for assistance with live animal imaging and operating the MRI system. We thank Dr. Robert Gros for assistance with blood pressure data collection (Western University).

## Declaration of conflicting interests

The author(s) declared no potential conflicts of interest with respect to the research, authorship, and/or publication of this article.

## Authors' contributions

JF, PMK and DGW designed the study. PMK induced the SMC  $K_{IR}2.1^{-/-}$  mice with tamoxifen. JF performed the electrophysiology and immunofluorescence experiments with analysis. MSMK performed the western blot experiments. GYM aided with immunofluorescence experiments and confirmatory electrophysiology experiments in wild-type mice. SEB performed the myography experiments. NH and DR aided with myography. PMK performed the blood pressure and MRI experiments. PMK completed analysis, statistics, and graphical presentation of the data. PMK, JF and DGW wrote the manuscript. WFJ, NRT and MTN contributed the superior epigastric artery study. MTN generated the transgenic mice. All authors approved the final version of the manuscript.

## Data availability statement

The data that support the findings of the study are included in this manuscript.

## ORCID iDs

Paulina M Kowalewska  <https://orcid.org/0000-0003-3231-3020>

Nathan R Tykocki  <https://orcid.org/0000-0001-5432-7656>

## Supplemental material

Supplemental material for this article is available online.

## References

1. Segal SS and Duling BR. Flow control among microvessels coordinated by intercellular conduction. *Science* 1986; 234: 868–870.
2. Zechariah A, Tran CHT, Hald BO, et al. Intercellular conduction optimizes arterial network function and conserves blood flow homeostasis during cerebrovascular challenges. *Arterioscler Thromb Vasc Biol* 2020; 40: 733–750.
3. Knot HJ, Zimmermann PA and Nelson MT. Extracellular K<sup>+</sup>-induced hyperpolarizations and dilations of rat coronary and cerebral arteries involve inward rectifier K<sup>+</sup> channels. *J Physiol* 1996; 492: 419–430.
4. Knot HJ and Nelson MT. Regulation of arterial diameter and wall [Ca<sup>2+</sup>] in cerebral arteries of rat by membrane potential and intravascular pressure. *J Physiol* 1998; 508: 199–209.
5. Zhang R, Zuckerman JH, Iwasaki K, et al. Autonomic neural control of dynamic cerebral autoregulation in humans. *Circulation* 2002; 106: 1814–1820.
6. Cole WC and Welsh DG. Role of myosin light chain kinase and myosin light chain phosphatase in the resistance arterial myogenic response to intravascular pressure. *Arch Biochem Biophys* 2011; 510: 160–173.
7. Thorneloe KS and Nelson MT. Ion channels in smooth muscle: regulators of intracellular calcium and contractility. *Can J Physiol Pharmacol* 2005; 83: 215–242.
8. Nelson MT and Quayle JM. Physiological roles and properties of potassium channels in arterial smooth muscle. *Am J Physiol Physiol* 1995; 268: C799–C822.
9. Quayle JM, Nelson MT and Standen NB. ATP-sensitive and inwardly rectifying potassium channels in smooth muscle. *Physiol Rev* 1997; 77: 1165–1232.
10. Bradley KK, Jaggar JH, Bonev AD, et al. Kir2.1 encodes the inward rectifier potassium channel in rat arterial smooth muscle cells. *J Physiol* 1999; 515: 639–651.
11. Hibino H, Inanobe A, Furutani K, et al. Inwardly rectifying potassium channels: their structure, function, and physiological roles. *Physiol Rev* 2010; 90: 291–366.
12. Quayle JM, McCarron JG, Brayden JE, et al. Inward rectifier K<sup>+</sup> currents in smooth muscle cells from rat resistance-sized cerebral arteries. *Am J Physiol Physiol* 1993; 265: C1363–C1370.
13. Shieh R-C, Chang J-C and Arreola J. J. Interaction of Ba<sup>2+</sup> with the pores of the cloned inward rectifier K<sup>+</sup> channels Kir2.1 expressed in *xenopus* oocytes. *Biophys J* 1998; 75: 2313–2322.
14. Wu B-N, Luykenaar KD, Brayden JE, et al. Hyposmotic challenge inhibits inward rectifying K<sup>+</sup> channels in cerebral arterial smooth muscle cells. *Am J Physiol Heart Circ Physiol* 2007; 292: H1085–H1094.
15. Sancho M, Fabris S, Hald BO, et al. Membrane lipid-K<sub>IR</sub>2.x channel interactions enable hemodynamic sensing in cerebral arteries. *Arterioscler Thromb Vasc Biol* 2019; 39: 1072–1087.
16. Schram G, Pourrier M, Wang Z, et al. Barium block of Kir2 and human cardiac inward rectifier currents: evidence for subunit-heteromeric contribution to native currents. *Cardiovasc Res* 2003; 59: 328–338.
17. Zaritsky JJ, Eckman DM, Wellman GC, et al. Targeted disruption of Kir2.1 and Kir2.2 genes reveals the essential role of the inwardly rectifying K<sup>+</sup> current in K<sup>+</sup>-mediated vasodilation. *Circ Res* 2000; 87: 160–166.
18. Wirth A, Benyó Z, Lukasova M, et al. G12-G13-LARG-mediated signaling in vascular smooth muscle is required for salt-induced hypertension. *Nat Med* 2008; 14: 64–68.
19. Sonkusare SK, Dalsgaard T, Bonev AD, et al. Inward rectifier potassium (Kir2.1) channels as end-stage boosters of endothelium-dependent vasodilators. *J Physiol* 2016; 594: 3271–3285.
20. Kilkenny C, Browne WJ, Cuthill IC, et al. Improving bioscience research reporting: the ARRIVE guidelines for reporting animal research. *PLoS Biol* 2010; 8: e1000412.
21. Nieves-Cintrón M, Tajada S, Santana LF, et al. Total internal reflection fluorescence microscopy in vascular smooth muscle. *Signal Transduct Smooth Muscle* 2018; 5: 87–103.
22. Hayoz S, Bradley V, Boerman EM, et al. Aging increases capacitance and spontaneous transient outward current amplitude of smooth muscle cells from murine superior epigastric arteries. *Am J Physiol Circ Physiol* 2014; 306: H1512–H1524.
23. Hayoz S, Pettis J, Bradley V, et al. Increased amplitude of inward rectifier K<sup>+</sup> currents with advanced age in smooth muscle cells of murine superior epigastric arteries. *Am J Physiol Circ Physiol* 2017; 312: H1203–H1214.
24. Mullan B, Pettis J and Jackson WF. T-type voltage-gated Ca<sup>2+</sup> channels do not contribute to the negative feedback regulation of myogenic tone in murine superior epigastric arteries. *Pharmacol Res Perspect* 2017; 5: e00320.
25. Westcott EB, Goodwin EL, Segal SS, et al. Function and expression of ryanodine receptors and inositol 1,4,5-trisphosphate receptors in smooth muscle cells of murine feed arteries and arterioles. *J Physiol* 2012; 590: 1849–1869.
26. Longden TA, Dabertrand F, Koide M, et al. Capillary K<sup>+</sup>-sensing initiates retrograde hyperpolarization to increase local cerebral blood flow. *Nat Neurosci* 2017; 20: 717–726.
27. Burns WR, Cohen KD and Jackson WF. K<sup>+</sup>-induced dilation of hamster cremasteric arterioles involves both the Na<sup>+</sup>/K<sup>+</sup>-ATPase and inward-rectifier K<sup>+</sup> channels. *Microcirculation* 2004; 11: 279–293.
28. Filosa JA, Bonev AD, Straub SV, et al. Local potassium signaling couples neuronal activity to vasodilation in the brain. *Nat Neurosci* 2006; 9: 1397–1403.
29. Smith PD, Brett SE, Luykenaar KD, et al. K<sub>IR</sub> channels function as electrical amplifiers in rat vascular smooth muscle. *J Physiol* 2008; 586: 1147–1160.
30. Dawes M, Sieniawska C, Delves T, et al. Barium reduces resting blood flow and inhibits potassium-induced vasodilation in the human forearm. *Circulation* 2002; 105: 1323–1328.
31. Jantzi MC, Brett SE, Jackson WF, Corteling R, et al. Inward rectifying potassium channels facilitate cell-

- to-cell communication in hamster retractor muscle feed arteries. *Am J Physiol Heart Circ Physiol* 2006; 291: H1319–H1328.
32. Liu GX, Derst C, Schlichthörl G, et al. Comparison of cloned Kir2 channels with native inward rectifier K<sup>+</sup> channels from guinea-pig cardiomyocytes. *J Physiol* 2001; 532: 115–126.
  33. Vanlandewijck M, He L, Mäe MA, et al. A molecular atlas of cell types and zonation in the brain vasculature. *Nature* 2018; 554: 475–480.
  34. He L, Vanlandewijck M, Mäe MA, et al. Single-cell RNA sequencing of mouse brain and lung vascular and vessel-associated cell types. *Sci Data* 2018; 5: 180160.
  35. Bochaton-Piallat M-L, Gabbiani F, Ropraz P, et al. Cultured aortic smooth muscle cells from newborn and adult rats show distinct cytoskeletal features. *Differentiation* 1992; 49: 175–185.
  36. Shanahan CM and Weissberg PL. Smooth muscle cell heterogeneity. *Arterioscler Thromb Vasc Biol* 1998; 18: 333–338.
  37. Adam PJ, Weissberg PL, Cary NR, et al. Polyubiquitin is a new phenotypic marker of contractile vascular smooth muscle cells. *Cardiovasc Res* 1997; 33: 416–421.
  38. Hoffman WE, Edelman G, Kochs E, et al. Cerebral autoregulation in awake versus isoflurane-anesthetized rats. *Anesth Analg* 1991; 73: 753–757.
  39. Wilde E, Aubdool AA, Thakore P, et al. Tail-cuff technique and its influence on Central blood pressure in the mouse. *Jaha* 2017; 6. doi:10.1161/JAHA.116.005204.
  40. Leonoudakis D, Conti LR, Anderson S, et al. Protein trafficking and anchoring complexes revealed by proteomic analysis of inward rectifier potassium channel (Kir2.x)-associated proteins. *J Biol Chem* 2004; 279: 22331–22346.